

Design and Optimization of Substrate Integrated Waveguide Bandpass Filter with T-Shape Slots Using Artificial Neural Networks

Ranjit K. Rayala^{*}, Ramasamy Pandeewari, and Singaravelu Raghavan

Abstract—The present paper describes a substrate integrated waveguide (SIW) bandpass filter with a T-shape slot on the upper layer, which exhibits a wide-band frequency response. The parameters of the filter are optimized by using Multi-Layer Perceptron artificial neural network (MLP-ANN) that uses Levenberg-Marquardt (LM) algorithm. A comparison is made between ANN optimized results and simulated results, and they result in minimum mean square error (MSE). A physical prototype is fabricated using printed circuit board (PCB) process, and measurements are conducted using the network analyzer. The measured results obtained agree well with the estimated ones. The filter shows a wide-band response with a transmission bandwidth of 8.96 GHz, ranging from 6.10 to 15.06 GHz with a fractional bandwidth of 81.4%. Furthermore, the insertion loss of the filter in the entire passband is varied from -0.4 dB to -0.2 dB, and the return loss is more than -10 dB.

1. INTRODUCTION

Technological innovations for the design and development of microwave and millimeter-wave components have evolved during the last few decades. The performance requirements for passive bandpass filters, a crucial component of these systems, are continually rising due to the rapid growth of such systems. Designing bandpass filters for microwave and millimetre wave frequencies is best done using SIW. Filters with various filtering properties, such as wide bandpass filters, multiband filters, and reconfigurable filters have been proposed [1]. SIW structures are made up of two rows of conducting vias embedded in a dielectric substrate that joins two parallel metal surfaces, allowing the use of rectangular waveguide components in planar form, as well as printed circuitry, active devices, and antennas. The current SIW technology advancements have been proposed in terms of SIW structure and component modelling, design, and implementation methods [2,3]. SIW has numerous advantages, including small size, simple fabrication, high efficiency, and ease of integration with other microwave and millimetre wave circuits [4]. In order to achieve wide band characteristics and size reduction, a bandpass filter with C and E slots in a folded substrate integrated waveguide (FSIW) and a quarter-mode substrate integrated waveguide (QMSIW) band-pass filter with an H-shaped slot have been proposed [5, 6]. A wide variety of applications of SIW are reported in recent years, viz. an approach of quasi-elliptic bandpass filters in SIW technology that uses mushroom shaped metallic resonators has been proposed [7]. SIW has also found profound applications in spatial filtering applications [8,9]. A wide bandpass filter with two resonators is formed by etching T-shape slots of different sizes on the top metal plane of the SIW structure, which provides significant improvements in size reduction and selectivity [10]. By embedding some sort of periodic structures into SIW, a super wide band bandpass filter has been realized [11].

T-shaped slot line spoof surface plasmon polaritons (SSPPs) have been built on the SIW structure in order to turn it into a substrate integrated plasmonic waveguide (SIPW) filter. The lower cutoff

Received 30 November 2022, Accepted 28 February 2023, Scheduled 15 March 2023

^{*} Corresponding author: Ranjit Kumar Rayala (ranjit.rayala@gmail.com).

The authors are with the Department of Electronics and Communication Engineering, National Institute of Technology, Tiruchirappalli, Trichy, Pin Code: 620015, India.

frequency can be changed by adjusting the SIW dimensions, while the upper cutoff frequency can be changed by adjusting the SSPP dimensions [12]. Based on SIW technology several filters in various topologies are designed efficiently and accurately [13]. The U-shape slots have been modeled on the SIW cavity, in order to turn it to a multiple mode resonator (MMR) that can achieve a wide passband and maintains a compact size [14]. The SIW bandpass filter has been designed using the rectangular waveguide resonator design method, which allows the optimization process to speed up by using initial configuration parameters [15].

Artificial neural network (ANN) has recently emerged as a powerful tool in microwave modelling and design [16, 17]. Because SIW components and RF circuits require more simulation time to optimise the design parameters, ANN was chosen as an alternative way to design microwave circuits and devices [18]. An artificial neural network (ANN) can be trained to learn nonlinear input-output relationships from the related data. After learning a task, these ANN models can be utilised to quickly respond to the task [19]. The deep neural network approach has been implemented into the area of high-dimensional microwave modelling, and an investigation has been performed to solve microwave modelling problems [20]. In order to solve the problems in multidimensional radio frequency and microwave passive devices, a new method of multi-dimensional neural network has been proposed [21].

In this paper a Multi-Layer Perceptron (MLP) ANN with two $1 \times 8 \times 1$ topologies are used to optimize the proposed SIW bandpass filter with T-shape slots. In order to train the neural network Levenberg-Marquart (LM) algorithm is used. The number of epochs used is 1000 in order to get minimum MSE, with a learning rate of 0.1. There is good agreement between the ANN results and CST Microwave studio simulation results.

The structure of this work is as follows. In Section 2, the SIW filter's design is explained. How to use neural networks to optimise filter parameters is explained in Section 3. The filter simulation process and its results are covered in Section 4. Information on the fabrication process and measuring setup is detailed in Section 5.

2. SIW BANDPASS FILTER DESIGN

2.1. SIW Design

The physical structure of SIW is as shown in Figure 1. The SIW structure consists of three layers as follows. Upper layer and bottom layer are made up of a material which is a perfect electric conductor (PEC), and middle layer is a dielectric material having some dielectric constant ϵ_r . Hence, the structure looks like that dielectric material is sandwiched between two PECs. The two side walls of the structure can be formed by rows of metallic vias on either side. The vias are placed into the waveguide from the lower PEC up to the upper PEC through the dielectric material.

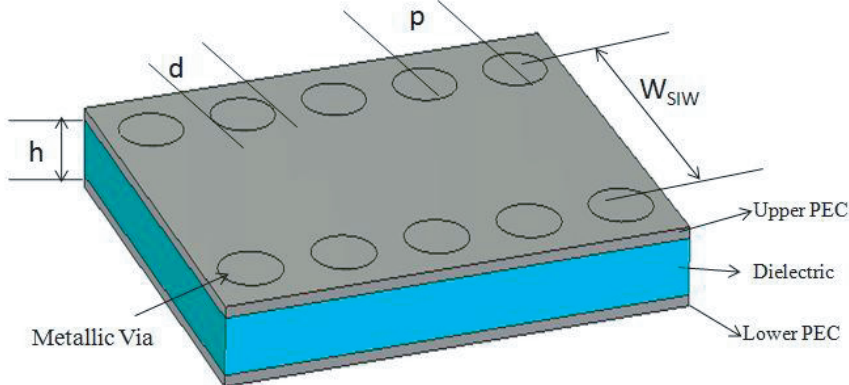


Figure 1. Physical structure of SIW.

2.2. Transition Formulas

We need some of the transition formulas, in order to transform classical waveguide into SIW. The classical rectangular waveguide (RWG) is as shown in Figure 2, where ‘ a ’ and ‘ b ’ indicate the width and height, respectively.

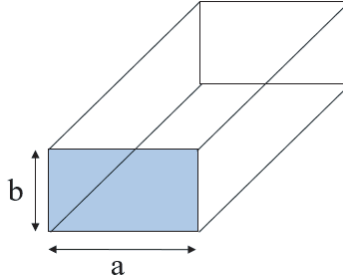


Figure 2. Conventional rectangular waveguide.

For this rectangular waveguide the cutoff frequency of any arbitrary mode is given by the formula as [2–4]:

$$f_c = \frac{c}{2\pi} \sqrt{\left(\frac{m\pi^2}{a^2} + \frac{n\pi^2}{b^2}\right)} \quad (1)$$

where ‘ a ’ and ‘ b ’ are dimensions of the RWG; ‘ c ’ is the speed of light; and ‘ m ’, ‘ n ’ are mode numbers. The cut-off frequency for the dominant mode (TE₁₀) is given by

$$f_c = \frac{c}{2a} \quad (2)$$

The width of SIW cavity can be determined by using the formula

$$W_{siw} = a_d + \frac{d^2}{0.95p} \quad (3)$$

where ‘ a'_d ’ is the width of dielectric filled waveguide and $a_d = \frac{a}{\sqrt{\epsilon_r}}$, ‘ d ’ the diameter, and ‘ p ’ the centre to centre separation between two adjacent vias. The two parameters ‘ d ’ and ‘ p ’ are selected in such a way that the following conditions must be satisfied.

$$d = \frac{\lambda_g}{5} \quad \text{and} \quad p < 2d \quad (4)$$

where

$$\lambda_g = \frac{c}{f\sqrt{\epsilon_r}}$$

λ_g = The guided wavelength,
 C = velocity of light in free space,
 f = operating frequency,
 ϵ_r = Dielectric constant

2.3. T-Shape Slot SIW Band Pass Filter Design Procedure

The proposed SIW bandpass filter with T-shape slots is as depicted in Figure 3. The dimensions of the proposed filter are as follows. The two parallel rows of metallic vias are separated by the width $W_{siw} = 13$ mm; the dielectric substrate length is $L = 30$ mm; the taper section length is $L_t = 14$ mm; the width of taper section is $W_t = 5.2$ mm; the microstrip line width is $W_{mst} = 1.8$ mm; diameter of the via is $d = 0.8$ mm; and these vias are placed with a separation distance or pitch of the vias, $p = 1.5$ mm.

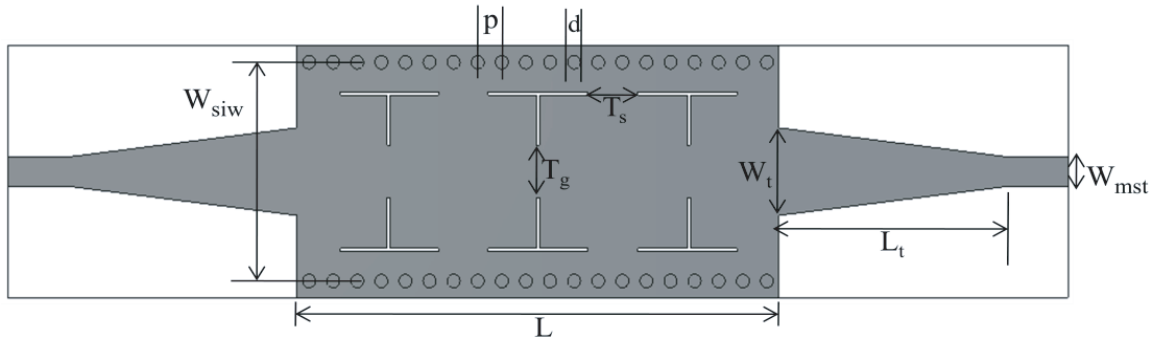


Figure 3. SIW bandpass filter with T-shape slots.

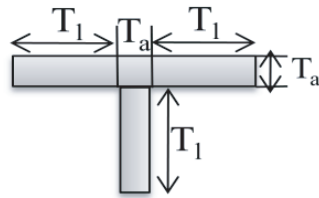


Figure 4. T shape slot.

On the upper PEC, T-shaped slots are etched. The dimensions of this T shape slot are as shown in Figure 4, with width $T_a = 0.2\text{ mm}$ and length of the arm $T_1 = 3\text{ mm}$. Three pairs of T shape slots are etched on the upper metallic surface, which face one another while keeping some gap of $T_g = 3.1\text{ mm}$ between them, and the distance between two slots is $T_s = 3.1\text{ mm}$.

3. PROPOSED SIW FILTER OPTIMIZATION USING ANN

3.1. Basic Architecture of Feed forward Artificial Neural Network (ANN)

Figure 5 illustrates the basic architecture of ANN. The most widely used neural network is Multi-Layer Perceptron (MLP) ANN, which consists of three phases: the input layer, the hidden layer, which itself contains a number of layers, and the output layer. In each and every layer, the neural network contains several nodes or base points, and these nodes are termed as ‘Neurons’. All these neurons are inter-

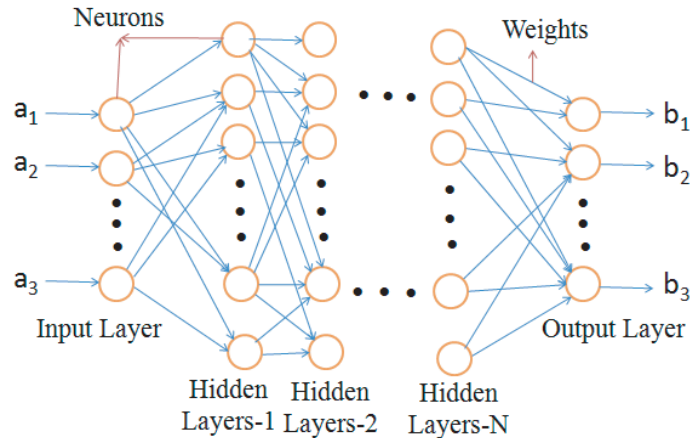


Figure 5. Basic architecture of ANN.

connected, and these links or connections are known as ‘Weights’. In MLP-ANN, the error was back propagated, in order to decrease the mean square error (MSE) for the subsequent epoch and so forth, and the weights are changed appropriately.

3.2. Optimization of Filter Dimensions Using ANN

The two neural networks that have been proposed consist of three layers: an input layer with one neuron, a hidden layer with eight neurons, and an output layer with one neuron ($1 \times 8 \times 1$). The first step in optimization procedure is the training process, and the second step is the testing process. In order to train and test the designed neural network, the training data and testing data are generated by using CST Microwave Studio. Tables 1(a) and 1(b) show the training data, and the Tables 2(a) and 2(b) show the testing data. The parameters T_g and W_{siw} of the proposed filter are optimized by using the designed neural network. The parameters W_{siw} and T_g are changed from 12.5 mm to 13.5 mm and 2.5 mm to 3.5 mm, respectively, to produce the necessary data for the neural network. The parameters T_g and W_{siw} act as input neurons, and the return loss (S_{11} in dB) acts as output neuron.

Levenberg-Marquardt (LM) algorithm is used in the optimization process. ‘trainlm’ is the most commonly used keyword in the MATLAB, which is the fastest back propagation algorithm. The number of epochs used is 1000 in order to get minimum MSE, with a learning rate of 0.1. Figure 6 shows the MSE plotted against the number of epochs. This curve shows how well the MLP-ANN trained.

Table 1. (a) Training data for T_g . (b) Training data for W_{siw} .

(a)			(b)		
S. No.	T_g (mm)	S_{11} (dB) (CST)	S. No.	W_{siw} (mm)	S_{11} (dB) (CST)
1	2.55	-11.85	1	12.65	-12.815
2	2.65	-13.09	2	12.75	-13.945
3	2.75	-14.281	3	12.85	-14.262
4	2.85	-14.954	4	12.95	-14.357
5	2.95	-15.608	5	13.05	-14.526
6	3.05	-15.859	6	13.15	-13.906
7	3.15	-15.951	7	13.25	-13.399
8	3.25	-14.474	8	13.35	-12.978
9	3.35	-13.090	9	13.45	-12.565
10	3.45	-11.870	10	13.55	-12.174

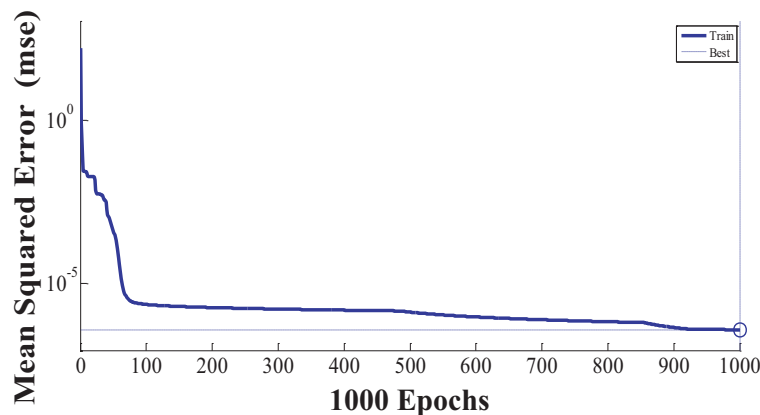


Figure 6. Training performance of proposed network.

Table 2. (a) Testing data for T_g . (b) Testing data for W_{siw} .

(a)

S. No.	T_g (mm)	S_{11} (dB) (CST)	S_{11} (dB) (ANN)	Mean Square Error
1	2.5	-11.360	-11.2288	0.0172
2	2.6	-12.506	-12.5013	0.0001
3	2.7	-13.712	-14.0334	0.1032
4	2.8	-14.823	-14.4022	0.1770
5	2.9	-15.427	-15.4693	0.0017
6	3.0	-15.759	-15.6861	0.0053
7	3.1	-15.966	-16.2192	0.0641
8	3.2	-14.874	-14.8704	0.0001
9	3.3	-13.347	-14.0907	0.5530
10	3.4	-12.019	-12.0702	0.0026

(b)

S. No.	W_{siw} (mm)	S_{11} (dB) (CST)	S_{11} (dB) (ANN)	Mean Square Error
1	12.6	-12.568	-12.7872	0.0480
2	12.7	-13.489	-13.5109	0.0004
3	12.8	-13.858	-14.1513	0.0860
4	12.9	-14.162	-14.2762	0.0130
5	13.0	-14.874	-14.4990	0.1406
6	13.1	-14.189	-14.4419	0.0639
7	13.2	-13.643	-13.4599	0.0335
8	13.3	-13.125	-13.3254	0.0401
9	13.4	-12.780	-12.7082	0.0051
10	13.5	-12.363	-12.2842	0.0062

After the proper testing of neural network, the results are summarized in Tables 2(a) and 2(b) with MSE. These test results reveal that the MLP-ANN output data and the S_{11} maximum obtained in the passband from CST are well agreed with each other with minimum MSE. The final optimized parameters are $T_g = 3.1$ mm and $W_{siw} = 13$ mm.

4. RESULTS AND DISCUSSION

The proposed wide bandpass filter was simulated using CST microwave studio. Figure 7 shows the performance characteristics of simulated S_{11} and S_{12} . From this graph at -3 dB we can observe that this filter has a wide transmission bandwidth of 8.96 GHz, and it is in between 6.10 GHz and 15.06 GHz having a fractional bandwidth of 81.45%. The IL in the entire in-band is varied from -0.4 dB to -0.2 dB, and the return loss is better than -10 dB. The filter offers a very good wide band response, and we can observe six resonant frequencies namely $f_1 = 6.2$ GHz, $f_2 = 7.2$ GHz, $f_3 = 8.5$ GHz, $f_4 = 10.4$ GHz, $f_5 = 12$ GHz, $f_6 = 14.22$ GHz, and the transmission zero (TZ) near the sixth resonant frequency (f_6) is helpful in order to get a good higher stopband. At -1 dB the filter offers a transmission bandwidth of 8.24 GHz ranging from 6.42 to 14.66 GHz with a fractional bandwidth of 74.9%.

Some of the parameters of the proposed filter were changed in order to perform the parametric study, and its graphical representation is as depicted in Figure 8. From the parametric study a set of values for S_{11} was obtained in order to train the artificial neural network (ANN). Figure 9 shows the electric field distribution of SIW filter with T-shape slots. The vertical colour ramps in the proposed filters represent the electric field strength (right side of Figure 9). The changes in the colour of the filter's

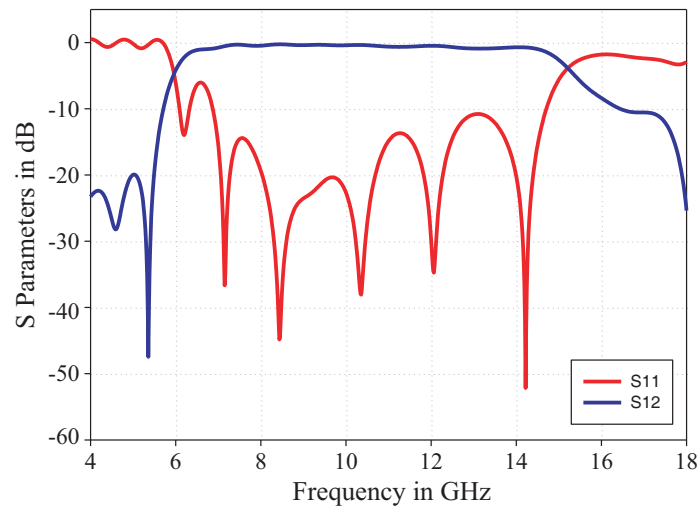


Figure 7. Frequency response of proposed filter.

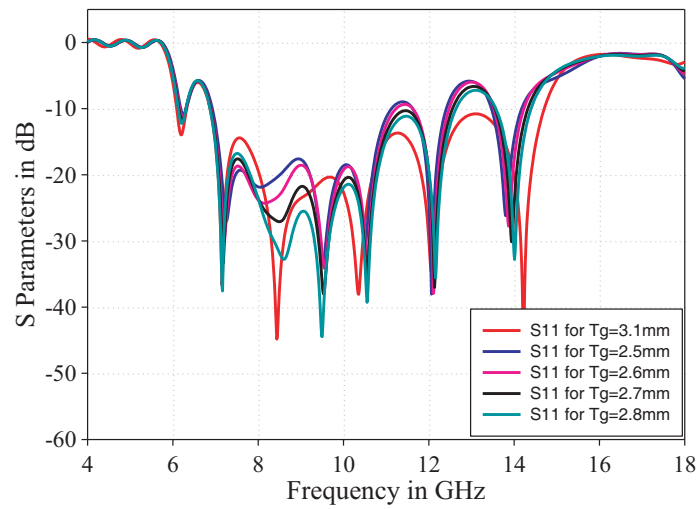


Figure 8. Parametric plot.

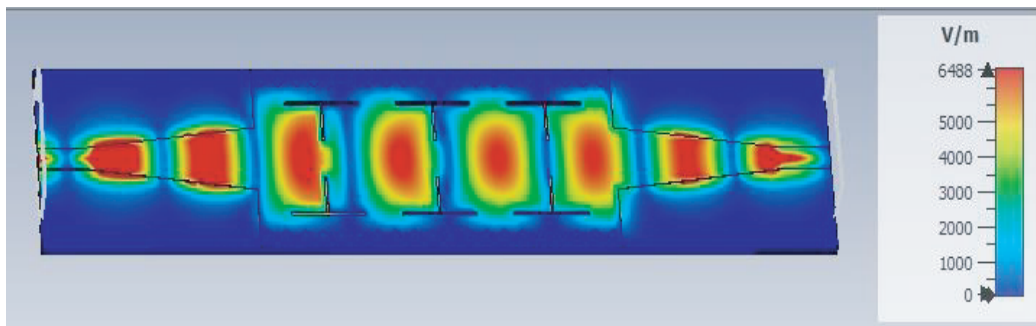


Figure 9. Electric field distribution.

upper surface in shades of red indicate an intensification of the electric field. The TE_{10} (dominant mode) behaviour of the proposed SIW filter is similar to that of a traditional rectangular waveguide.

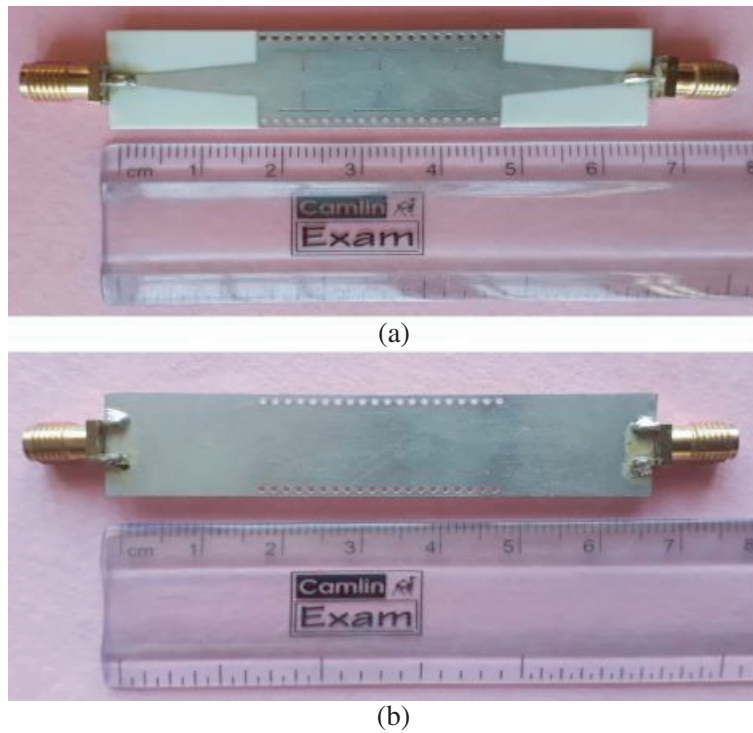


Figure 10. Fabricated filter models. (a) Top view. (b) Bottom view.

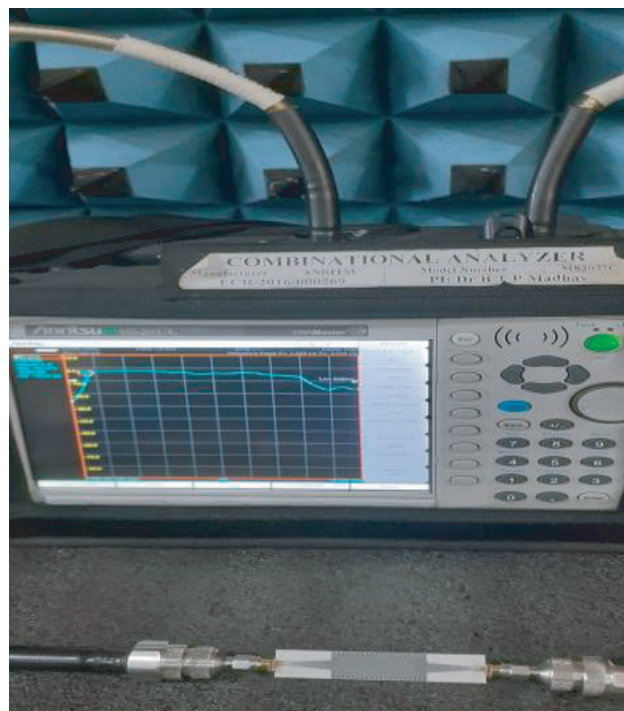


Figure 11. Measurement setup.

5. FABRICATION AND MEASUREMENT

The proposed wide band bandpass filter which is fabricated using simple PCB design process and the prototype is shown in Figure 10. For the fabrication of this filter Rogers RO4003C is used as a dielectric material with dielectric constant $\epsilon_r = 3.55$ and a magnetic loss tangent of $\tan(\delta) = 0.0027$, and the material height is $h = 0.81$ mm. With the optimized values mentioned above the filter is fabricated, and the front view and bottom side is shown in Figure 10. Figure 11 depicts the measurement using the Combinational Analyzer (Anritsu-MS2037C).

Figure 12 shows the plot of measured and simulated results, and it shows a wide band response. At band centre frequency 11 GHz, the simulated and measured transmission coefficients S_{12} show an insertion loss about -0.3 dB and -1.75 dB, respectively. This energy loss is mainly due to dielectric loss and SMA connectors used.

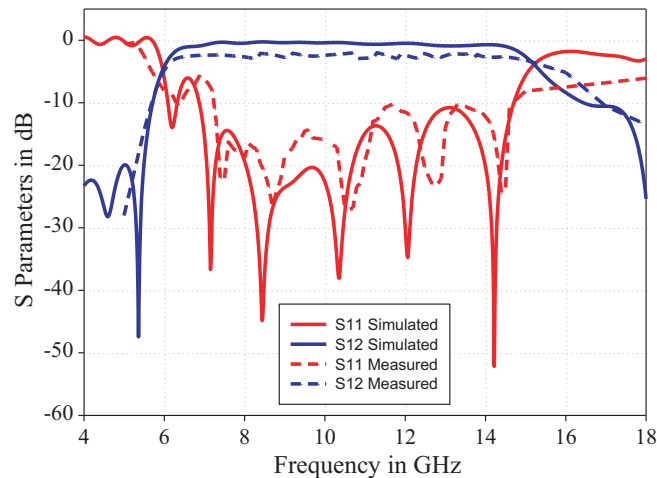


Figure 12. Plot of simulated results and measured results.

6. CONCLUSION

A wide band SIW bandpass filter with T-shaped slots is presented in this paper. MLP-ANN is used to optimize the dimensions of proposed filter, such as T_g and W_{siw} . Levenberg-Marquardt (LM) algorithm is used with a learning rate of 0.1. The full-wave simulated design parameters of the proposed filter are optimized with ANN. The simulated results are in good agreement with the ANN optimized values. A prototype of the proposed model is fabricated and tested experimentally. The -3 dB bandwidth is 8.96 GHz, with the fractional bandwidth of 81.4% and insertion loss varied from -0.4 dB to -0.2 dB, and better than -10.0 dB return loss is achieved. It is observed that the neural networks are very helpful in finding the parameters of the microwave components and circuits with better accuracy. The complex simulations and computational time are also reduced in designing the circuit.

REFERENCES

1. Chen, X. and K. Wu, "Substrate integrated waveguide filters: Design techniques and structure innovations," *IEEE Microwave Magazine*, Vol. 15, No. 6, 121–133, 2014.
2. Maurizio, B., G. Apostolos, and W. Ke, "Review of substrate-integrated waveguide circuits and antennas," *IET Microwaves, Antennas and Propagation*, Vol. 5, No. 8, 909–920, 2011.
3. Krushna Kanth, V. and S. Raghavan, "EM design and analysis of a substrate integrated waveguide based on a frequency-selective surface for millimeter wave radar application," *J. Comput. Electron.*, Vol.18, 189–196, 2019.

4. Deslandes, D. and K. Wu, "Single-substrate integration technique of planar circuits and waveguide filters," *IEEE Transactions on Microwave Theory and Techniques*, Vol. 51, No. 2, 593–596, 2003.
5. Muchhal, N., A. Chakraborty, M. Vishwakarma, and S. Srivastava, "Slotted folded substrate integrated waveguide band pass filter with enhanced bandwidth for Ku/K band applications," *Progress In Electromagnetics Research M*, Vol. 70, 51–60, 2018.
6. Wu, Y.-D., G. H. Li, W. Yang, and X. Yang, "Design of compact wideband QMSIW band-pass filter with improved stopband," *Progress In Electromagnetics Research Letters*, Vol. 65, 75–79, 2017.
7. Tomassoni, C., L. Silvestri, M. Bozzi, and L. Perregrini, "Substrate-integrated waveguide filters based on mushroom-shaped resonators," *International Journal of Microwave and Wireless Technologies*, Vol. 8, No. 4–5, 741–749, 2016.
8. Kanth, V. K. and S. V. Raghavan, "Design and development of angularly stable and polarisation rotating FSS radome based on substrate-integrated waveguide technology," *IET Microwaves, Antennas and Propagation*, Vol. 13, No. 4, 478–484, 2019.
9. Kanth, V. K. and S. Raghavan, "Design of SIW cavity models to control the bandwidth of frequency selective surface," *IET Microwaves, Antennas and Propagation*, Vol. 13, No. 14, 2515–2524, 2019.
10. Danaeian, M., A. G. Ashkezari, K. Afrooz, and A. Hakimi, "A compact wide bandpass filter based on Substrate Integrated Waveguide (SIW) structure," *Journal of Communication Engineering*, 2015.
11. Hao, Z.-C., W. Hong, J.-X. Chen, X.-P. Chen, and K. Wu, "Compact super-wide bandpass Substrate Integrated Waveguide (SIW) filters," *IEEE Transactions on Microwave Theory and Techniques*, Vol. 53, No. 9, 2968–2977, 2005.
12. Chen, P., L. Li, K. Yang, and F. Hua, "Design of substrate integrated plasmonic waveguide bandpass filter with T-shaped spoof surface Plasmon polaritons," *Electromagnetics*, Vol. 40, No. 8, 563–575, 2020.
13. Caballero, E. D., H. Esteban, A. Belenguer, V. E. Boria, J. V. Morro, and J. Cascon, "Efficient design of substrate integrated waveguide filters using a hybrid mom/mm analysis method and efficient rectangular waveguide design tools," *International Conference on Electromagnetics in Advanced Applications*, 456–459, 2011.
14. Chen, R. S., S. Wong, L. Zhu, and Q. Chu, "Wideband bandpass filter using U-slotted Substrate Integrated Waveguide (SIW) cavities," *IEEE Microwave and Wireless Components Letters*, Vol. 25, No. 1, 1–3, 2015.
15. Wang, Y., Y. Fu, Q. Liu, and S. Dong, "Design of a substrate integrated waveguide bandpass filter using in microwave communication systems," *International Conference on Microwave and Millimeter Wave, Technology*, 1952–1954, Chengdu, China, 2010.
16. Zhang, Q.-J., K. C. Gupta, and V. K. Devabhaktuni, "Artificial neural networks for RF and microwave design — From theory to practice," *IEEE Transactions on Microwave Theory and Techniques*, Vol. 51, No. 4, 1339–1350, 2003.
17. Rayas-Sanchez, J. E., "EM-based optimization of microwave circuits using artificial neural networks: The state-of-the-art," *IEEE Transactions on Microwave Theory and Techniques*, Vol. 52, No. 1, 420–435, 2004.
18. Angiulli, G., E. Arnieri, D. De Carlo, and G. Amendola, "Feed forward neural network characterization of circular SIW resonators," *IEEE Antennas and Propagation Society International Symposium*, 1–4, San Diego, CA, USA, 2008.
19. Devabhaktuni, V. K., M. C. E. Yagoub, Y. Fang, J. Xu, and Q.-J. Zhan, "Neural networks for microwave modeling: Model development issues and nonlinear modeling techniques," *Int. J. RF Microwave Comput.-Aided Eng.*, Vol. 11, 4–21, 2001.
20. Jin, J., C. Zhang, F. Feng, W. Na, J. Ma, and Q. Zhang, "Deep neural network technique for high-dimensional microwave modeling and applications to parameter extraction of microwave filters," *IEEE Transactions on Microwave Theory and Techniques*, Vol. 67, No. 10, 4140–4155, 2019.
21. Fan, P., R. G. Zhou, and Z. B. Chang, "Novel neural network modelling method and applications," *Int. J. RF Microwave Comput.-Aided Eng.*, Vol. 25, No. 9, 769–779, 2015.